

10-1996

Refinement of the RLAB Color Space

Mark Fairchild

Rochester Institute of Technology

Follow this and additional works at: <http://scholarworks.rit.edu/article>

Recommended Citation

Fairchild, M. D. (1996), Refinement of the RLAB color space. *Color Res. Appl.*, 21: 338–346. DOI: 10.1002/(SICI)1520-6378(199610)21:5<338::AID-COL3>3.0.CO;2-Z

This Article is brought to you for free and open access by RIT Scholar Works. It has been accepted for inclusion in Articles by an authorized administrator of RIT Scholar Works. For more information, please contact ritscholarworks@rit.edu.

Mark D. Fairchild

Munsell Color Science Laboratory

Center for Imaging Science

Rochester Institute of Technology

54 Lomb Memorial Drive

Rochester, New York 14623-5604

Refinement of the RLAB Color Space

The prediction of color appearance using the RLAB color space has been tested for a variety of viewing conditions and stimulus types. These tests have shown that RLAB performs well for complex stimuli and not-so-well for simple stimuli. This article reviews the various psychophysical results, interprets their differences, and describes evolutionary enhancements to the RLAB model that simplify it and improve its performance.

Key Words: Color Appearance, Color Spaces, Color-Appearance Models, Psychophysics

INTRODUCTION

The accurate reproduction of color images in different media has a number of requirements.¹ One of the most notable is the need to specify and reproduce color appearance across a range of media and viewing conditions. This cannot be accomplished using traditional colorimetry, which is only capable of predicting color matches under identical viewing conditions for the original and reproduction. When viewing conditions such as the luminance level, white-point chromaticity, surround relative luminance, and cognitive interpretation of the medium vary, a color-appearance model is necessary to predict the appropriate image transformation to produce an image that closely resembles the color appearances of the original.

The RLAB color-appearance space was developed by Fairchild and Berns for cross-media color reproduction applications in which images are reproduced with differing white points, luminance levels, and/or surrounds.² Since its development, the RLAB space has been subjected to a series of psychophysical comparisons with other color-appearance models. This paper reviews the RLAB space, briefly describes the results of some visual evaluations of its performance, and outlines the derivation of a revised version of RLAB. The revisions result in a simpler formulation of RLAB with performance equal to or better than the original in all applications evaluated to date.

The **Collins COBUILD English Language Dictionary** provides the following definition:

refinement: an alteration or addition that you make to something in order to make it more efficient or easier to use.

This definition aptly describes the objectives of this article. The equations that define the RLAB model have been refined. The result is a model that is more efficient, is easier to use and performs the same as the original model in most situations and significantly better in some.

OVERVIEW OF RLAB

A detailed derivation of the original RLAB equations is available in reference 2. A descriptive summary of the philosophy and implementation of the RLAB color-appearance space is given below.

RLAB was derived to have color-appearance predictors similar to those of the CIELAB color space.³ RLAB includes predictors of lightness, L^R , redness-greenness, a^R , yellowness-blueness, b^R , chroma, C^R , and hue angle, h^R . These appearance predictors are calculated using equations virtually identical to the CIELAB equations after the stimulus tristimulus values are transformed to the corresponding tristimulus values for the reference viewing condition (D65, 318 cd/m², hard copy). The transformation is accomplished using a modified von Kries-type chromatic adaptation transformation previously formulated by Fairchild.⁴ The end result is that the RLAB color space is identical to (and takes advantage of the excellent

performance of) the CIELAB color space for the reference viewing conditions and average surround relative luminance. However, for other viewing conditions, the more accurate chromatic-adaptation transform replaces the normalization of tristimulus values inherent in the CIELAB equations.

The chromatic-adaptation transform utilized in RLAB has several unique features. The first is the capability to predict incomplete levels of chromatic adaptation that allow highly chromatic "white-points" to retain some of their chromatic appearance. In addition, the incomplete-chromatic-adaptation feature can be turned on or off depending on whether cognitive "discounting-the-illuminant" mechanisms are active. These mechanisms are active when viewing hard-copy images in an illuminated environment and inactive when viewing soft-copy images. A final unique feature of RLAB is a matrix in the transformation that models interaction between the cone types allowing the prediction of luminance-dependent appearance effects such as the Hunt effect (increase in perceived colorfulness with luminance).

Another aspect of the RLAB model is that the power-function nonlinearities in the CIELAB equations (cube root) are allowed to vary depending on the image-surround conditions.⁵ This models the change in image contrast caused by changes in the relative luminance of the image surround. For example, the dark surround in which projected slides are typically viewed causes the perceived contrast to be lower than if the same image luminances were presented in an average surround as is typical of a printed image.

VISUAL EVALUATION OF RLAB

A series of experiments has been undertaken to visually evaluate the performance of various color-appearance models under a variety of viewing conditions using both complex stimuli (images) and simple color patches. This section reviews and summarizes the results of four such studies. Comparison of the RLAB color-appearance model to the other models in these experiments has provided a greater understanding of its relative strengths and weaknesses.

Print-To-Print Image Reproduction

Experiment 1 examined the reproduction of printed images viewed under different light sources at different luminance levels. Details of this experiment were described by Kim *et al.*⁶ Four pictorial images were used in this experiment. The originals were viewed under a CIE illuminant A simulator at a luminance level (white) of 214 cd/m². Reproductions were viewed under fluorescent CIE illuminant D65 simulators at one of three different luminance levels (71, 214, and 642 cd/m²). The reproductions were produced by applying color-appearance transformations as described by each of eight models. The reproductions were viewed pairwise in every possible combination and 30 observers were asked to choose which image in each pair was a better reproduction of the original. The data were then analyzed using Thurstone's Law of Comparative Judgements to derive interval scales of

model performance. Confidence limits were also calculated about each of the scale values. The images were viewed using a successive-*Ganzfeld* haploscopic viewing technique.⁷ The rank order of each model's performance (averaged over all images and conditions) is given in Table I. Models that did not perform significantly differently from one another are given identical ranks. Only the results for the five appearance models common to all of the experiments are given in table I. In experiment 1, the RLAB, CIELAB, Hunt, and von Kries models all performed similarly, while the Nayatani model performed significantly worse. The other three models performed worse than each of these five and were not included in further experiments.

Simple Object-Color Reproduction

Experiment 2 was virtually identical to experiment 1 with the exception that simple color patches, viewed one at a time, on gray backgrounds were used as stimuli rather than pictorial images. Details of this experiment were described by Pirrotta.¹¹ Ten different original colors, chosen to maximize differences between the appearance-model predictions, were used. The originals were viewed under a CIE illuminant A simulator at a luminance level (white) of 73 cd/m². Reproductions were viewed under fluorescent CIE illuminant D65 simulators at a luminance of 763 cd/m². Nine different color-appearance transformations were evaluated using the same experimental procedure and analysis as experiment 1 and viewed via the successive-

Ganzfeld haploscopic technique⁷ by 26 observers. The rank order of each model's performance (averaged over all colored patches) is given in Table I. In experiment 2, the Hunt model performed significantly better than the others followed by the Nayatani, von Kries, and CIELAB models with similar performance. The RLAB model performed significantly worse than all of the other models in this experiment. It is of interest that the RLAB model performed best for pictorial images and worst for simple color patches under similar experimental conditions.

Further analysis of the RLAB model revealed that it introduced an unwanted shift in the lightness of the color samples upon changes in luminance level. This resulted in the poor performance of RLAB for the simple color patches. This problem was not apparent in the experiments using pictorial images since the lightness shift occurred for all of the image colors such that the image contrast was properly reproduced. This deficiency in the RLAB model was traced to the **C** matrix, which models interactions between the cone types. The problem is corrected by removal of the **C** matrix in the revised formulation of RLAB¹² given below.

Print-To-CRT Image Reproduction

Experiment 3 examined the performance of five color-appearance transformations for reproductions of printed original images as CRT-displayed images. The experiment was carried out using five different viewing techniques to determine which was most appropriate for such

comparisons.^{13,14} A memory matching technique was determined to be the most appropriate. Thus, the memory-matching results are summarized below. Five different pictorial images were used as originals. In one session, the originals were viewed under a fluorescent CIE illuminant D50 simulator. In the second session, the originals were viewed under a CIE illuminant A simulator. The reproductions were viewed on a CRT monitor with CIE illuminant D65 white-point chromaticities. The luminance of white for all conditions was 75 cd/m^2 . Both the originals and reproductions were viewed with white borders, gray backgrounds, and dark surrounds. Fifteen observers took part in this experiment. A paired-comparison experiment with data analysis similar to the first two experiments was used. The model-performance rank order (averaged over images and print white points) is given in Table I. This experiment proved to be the most sensitive test of model performance with each model performing significantly differently than the others. The order of performance from best to worst was RLAB, CIELAB, von Kries, Hunt, Nayatani. The problems exhibited by RLAB in experiment 2 were not apparent in this experiment due to the use of equal luminance levels and complex images.

CRT-To-Projected Slide Reproduction

Experiment 4 was carried out in a manner similar to experiment 3. However the original images were presented on a CRT display with white-point chromaticities of either CIE illuminant D65 at 53 cd/m^2 or CIE illuminant D93

at 60 cd/m^2 and the reproductions were projected 35mm transparencies with a white-point correlated color temperature of 3863K at a luminance of 109 cd/m^2 . The CRT images were viewed in a dim surround of office lighting (cool-white fluorescent) and the projected transparencies were viewed in a dark surround to test the models' abilities to predict surround effects. Fifteen observers completed the experiment. The data were collected using a memory matching technique and analyzed in a way similar to the first 3 experiments. The Nayatani model was excluded from the psychophysical experiments since the images produced by it were clearly unacceptable. The rank order results (averaged over 3 pictorial images) are given in Table I. The RLAB model performed best followed by both CIELAB and von Kries, Hunt performed the worst of the models evaluated. Details of this experiment are described by Fairchild *et al.*¹⁵

Image and Color Dependence

It should be noted that the results described in this paper are the overall average results for each experiment. There are many details worthy of further investigation in the complete results of each experiment. For example, the performance of the models is typically somewhat image dependent. Usually the rank order of the models remains approximately the same, but occasionally more drastic dependencies can be noted. For example, CIELAB performs poorly for blue hues. Thus if an experiment were designed using images that all had a preponderance of blue, the performance of

CIELAB would likely be much worse than indicated by the results summarized above. The same is also true for experiment 2 in which simple color patches were used. The models' performance differed for the various colors investigated. This color dependency is likely to be a major cause of the observed image dependency.

REFINEMENT OF THE RLAB EQUATIONS:

The RLAB model performs as well as, or better than, all of the other color-appearance transformations in the experiments using image stimuli. Since the original objective in the derivation of RLAB was to develop a simple model that would perform at least as well as more complicated models in color reproduction applications it seems that it has been successful. However, the poor performance of RLAB in experiment 2 highlighted a flaw in the model that could easily be corrected without affecting the good performance in the other experiments. In addition, further simplifications of the equations have been derived that allow easier implementation and inversion of the model (both necessary for imaging applications). This was accomplished by replacing the conditional linear/power functions of the CIELAB equations with approximately equivalent simple power functions that do not require the conditional implementation and its complex inversion. Further flexibility was added to RLAB by allowing the cognitive "discounting-the-illuminant" mechanisms to be partially active. This is likely the case in situations such as large projected transparencies in a

darkened room. Two of the intermediate matrices in the model have been renormalized resulting in a significant simplification of several equations and greater computational efficiency by reducing of the number of divisions required. Lastly, the capability to express hue as percentage combinations of the unique hues was added to provide a more accurate definition of perceived hue. These changes are detailed below in the new RLAB equations.

C Matrix

The chromatic-adaptation transformation incorporated in the original RLAB equations consisted of a series of three matrix multiplications. The first was a matrix, **M**, to convert from CIE tristimulus values, XYZ, to cone excitations, LMS. The second matrix, **A**, was a diagonal matrix representing a modified von Kries gain control acting independently on each of the three cone excitations. The third matrix, **C**, had values of 1.0 along the diagonal while all of the off-diagonal terms were equal and a function of the adapting luminance level. The **C** matrix provided for luminance-dependent interactions between the three cone types allowing the model to predict luminance-dependent color-appearance effects such as the Hunt and Stevens effects.

While the **C** matrix was effective, it also introduced an overall lightness shift in predicted corresponding colors across changes in luminance level. This shift is not observed experimentally and is what led to the poor performance of RLAB in experiment 2. This weakness in the original RLAB

equations did not show up in other experiments because they were either done at constant luminance (in which case the **C** matrix has no effect) or they were done with complex images (in which case the overall image contrast masked an offset in lightness).

It was decided that the **C** matrix was more detrimental than beneficial and it was therefore deleted from the revised model. While this means that the new RLAB model cannot predict the Hunt and Stevens effects, this is not important in practical situations. Often, luminance levels are nearly equal for originals and reproductions and these effects will not be apparent. In other cases, one is limited by the gamut of the reproduction device and the increases in luminance and chromatic contrast required for reproduction at lower luminance levels cannot be physically produced. Thus, the practical issue of gamut mapping will negate the prediction of these effects. Alternatively, when reproducing an image at higher luminance levels, a model predicting these effects would underutilize the output gamut and thus produce sub-optimal results. Therefore the new chromatic-adaptation transformation includes only 2 matrices, **M** and **A**.

Partial Discounting-the-Illuminant

In the original RLAB model, incomplete chromatic adaptation was predicted using a factor, p , in the von Kries coefficients. This factor varies about 1.0 (complete adaptation) depending on the chromaticity and luminance of the adapting stimulus. In cases where observers could invoke cognitive

mechanisms and thus “discount the illuminant,” the p factor was set equal to 1.0 indicating that chromatic adaptation was, in effect, complete. Typically the calculated p value was used for soft-copy displays and a value of 1.0 was used for hard-copy displays in which the observer could interpret the illumination environment.

In some cases, observers are in an intermediate state of adaptation in which they are partially discounting the illuminant. This might happen, for example, when large projected transparencies are viewed in a darkened room and observers tend to perceive the image as if it is an illuminated environment. In fact, color transparency films intended for projection using tungsten sources are intentionally designed to produce bluish images of neutral colors such that they appear gray when the observer is adapted to the tungsten projector light.¹⁶ In such cases, it would be convenient to use intermediate values that fall between p and 1.0. To allow such situations to be appropriately modeled, a D parameter was added to describe the level of discounting the illuminant as illustrated in Eq. 1. When there is no discounting-the-illuminant D equals 0.0 and Eq. 1 reduces to p .

$$p + D(1.0 - p) \tag{1}$$

When there is complete discounting-the-illuminant D equals 1.0 and Eq. 1 reduces to 1.0. These extreme cases are identical to the original RLAB equations. The new equation allows the possibility of intermediate values.

Simplified Power Functions

The original RLAB model used the CIELAB equations for the compressive nonlinearity in the lightness and chroma scales. These equations follow a power function for most of their range and then switch to a linear function to avoid negative values of L^* as illustrated in Eq. 2. These equations require a

$$\begin{aligned} f(x) &= (x)^{1/3} &> 0.008856 \\ f(x) &= 7.787(x) + 16/116 &0.008856 \end{aligned} \quad (2)$$

check of the initial values and then a decision regarding which function to use. This is not difficult for a few computations, but becomes more of a burden when processing large amounts of image data. In addition, since the RLAB model provides different exponents for the power function for different surround conditions, there are also different sets of test conditions and corresponding linear functions for each surround condition (requiring the derivation of a new transition point and linear function for the low end of the range). This situation makes inversion of the model quite cumbersome and the use of custom exponents extremely difficult.

To avoid the difficulties described above the compressive nonlinearities of the form described in Eq. 2 were replaced with simple power functions as illustrated in Eqs. 11-13. These simplify model inversion, increase computational efficiency, and allow intermediate, or custom, exponents for particular applications. The nominal exponents were derived by finding the power functions that best fit the combination functions of Eq. 2 for the 3 surround conditions recommended in the original RLAB model.

The fits were quite satisfactory. However there are some systematic discrepancies between the old and new functions. Figure 1 illustrates the differences between the new and original compression functions in terms of predicted lightness differences for dark, dim, and average surrounds. These discrepancies are small compared to the uncertainty in visual color-appearance judgements.¹⁷ Also, the relationships between the functions for various surround conditions have not changed. Thus if one uses the RLAB model to produce a reproduction across a change in surround relative luminance, the results of the new and old equations will be indistinguishable. It should be noted that changing these functions required a change in the scaling factors (100, 430, and 170) in Eqs. 11-13 below in order to retain scales similar to CIELAB.

Renormalization Of Matrices

Determination of the degree of chromatic adaptation requires the calculation of fundamental chromaticity coordinates relative to an equal-energy illuminant. This requires normalization of the cone excitations to the cone excitations for the equal-energy illuminant. Since this normalization is always performed, it is possible to simplify the equations by incorporating the normalization into the **M** matrix that is used for the conversion from XYZ to LMS. This new **M** matrix has been incorporated in Eq. 4 below and results in a simplification of Eq. 8 when compared to the original RLAB equations.

The conversion from reference tristimulus values to the L^R , a^R , and b^R coordinates requires a normalization to the tristimulus values of the reference illuminant, CIE illuminant D65. Again this normalization is always performed so it can be incorporated in a renormalization of the \mathbf{R} matrix that is used to transform to the reference tristimulus values. The new \mathbf{R} matrix (calculated using the new adaptation transform and then normalized) is given in Eq. 10. This normalization results in a significant simplification of Eqs. 11-13 when compared to the original RLAB equations.

Together, these two matrix renormalizations remove a total of nine division operations from the RLAB model while making no change in the calculated values. This is a substantial computational savings and a significant simplification in the equations.

SUMMARY OF RLAB EQUATIONS

The following equations describe the forward implementation of the new RLAB equations. One begins with a conversion from CIE tristimulus values ($Y = 100$ for white) to fundamental tristimulus values as illustrated in Eqs. 3 and 4. All CIE tristimulus values are calculated using the CIE 1931 Standard Colorimetric Observer (2°).

$$\begin{pmatrix} L \\ M \\ S \end{pmatrix} = \mathbf{M} \begin{pmatrix} X \\ Y \\ Z \end{pmatrix} \quad (3)$$

$$\mathbf{M} = \begin{vmatrix} 0.3897 & 0.6890 & -0.0787 \\ -0.2298 & 1.1834 & 0.0464 \\ 0.0 & 0.0 & 1.0000 \end{vmatrix} \quad (4)$$

The next step is calculation of the \mathbf{A} matrix that is used to model the chromatic adaptation transformation.

$$\mathbf{A} = \begin{vmatrix} a_L & 0.0 & 0.0 \\ 0.0 & a_M & 0.0 \\ 0.0 & 0.0 & a_S \end{vmatrix} \quad (5)$$

$$a_L = \frac{p_L + D(1.0 - p_L)}{L_n} \quad (6)$$

$$p_L = \frac{(1.0 + Y_n^{1/3} + \ell_E)}{(1.0 + Y_n^{1/3} + 1.0/\ell_E)} \quad (7)$$

$$\ell_E = \frac{3.0L_n}{L_n + M_n + S_n} \quad (8)$$

The a terms for the short- (S) and middle-wavelength (M) sensitive systems are derived in a similar fashion using functions analogous to Eqs. 6-8. Y_n is the absolute adapting luminance in cd/m^2 . Terms with n subscripts refer to values for the adapting stimulus derived from relative tristimulus values. The D factor was added to Eq. 6 to allow various proportions of cognitive "discounting-the-illuminant". D should be set equal to 1.0 for hard-copy images, 0.0 for soft-copy displays, and an intermediate value for situations such as projected transparencies in completely darkened rooms. The exact choice of intermediate values will depend upon the specific viewing conditions. Katoh¹⁸ has illustrated an example of intermediate adaptation in direct comparison between soft- and hard-copy displays and Fairchild¹⁹ has

reported a case of intermediate discounting-the-illuminant for a soft-copy display. When no visual data are available and an intermediate value is necessary, a value of 0.5 should be chosen and refined with experience.

After the **A** matrix is calculated, the tristimulus values for a stimulus color are converted to corresponding tristimulus values under the reference viewing conditions using Eqs. 9 and 10.

$$\begin{bmatrix} X_{\text{ref}} \\ Y_{\text{ref}} \\ Z_{\text{ref}} \end{bmatrix} = \mathbf{R} \mathbf{A} \mathbf{M} \begin{bmatrix} X \\ Y \\ Z \end{bmatrix} \quad (9)$$

$$\mathbf{R} = \begin{bmatrix} 1.9569 & -1.1882 & 0.2313 \\ 0.3612 & 0.6388 & 0.0 \\ 0.0 & 0.0 & 1.0000 \end{bmatrix} \quad (10)$$

The RLAB coordinates are then calculated using Eqs. 11-15.

$$L^R = 100(Y_{\text{ref}}) \quad (11)$$

$$a^R = 430[(X_{\text{ref}}) - (Y_{\text{ref}})] \quad (12)$$

$$b^R = 170[(Y_{\text{ref}}) - (Z_{\text{ref}})] \quad (13)$$

$$C^R = \sqrt{(a^R)^2 + (b^R)^2} \quad (14)$$

$$h^R = \tan^{-1}(b^R / a^R) \quad (15)$$

Equations 11-13 have been simplified as described above to avoid complexities in the implementation and inversion of the CIELAB-style equations. The exponents have changed slightly, but their ratios have remained the same. For an average surround $s = 1/2.3$, for a dim surround $s = 1/2.9$, and for a dark surround $s = 1/3.5$. As a nominal definition, a dark

surround is considered essentially zero luminance, a dim surround is considered a relative luminance less than 20 percent of white in the image, and an average surround is considered a relative luminance equal to or greater than 20 percent of the image white. In some applications, it might be desired to use intermediate values for the exponents in order to model less severe changes in surround relative luminance. This requires no more than a substitution in the new RLAB equations. In addition, it might be desirable to use different exponents on the lightness, L^R , dimension than on the chromatic, a^R and b^R , dimensions.⁵ This can also be easily accommodated.

Hue composition has been used in previously published color-appearance models^{9,10} to facilitate a natural specification of the hue attribute. This is useful when testing a color-appearance model against magnitude estimation data¹⁷ and when it is desired to reproduce a named hue. Hue composition, H^R , can be calculated via linear interpolation of the values in Table II. These were derived based on the notation of the Swedish Natural Color System (NCS)²⁰ and are illustrated in Fig. 2. The NCS notations are based on visual evaluation by a large number of observers.²¹ Figure 2 is a useful visualization of the loci of the unique hues since they do not correspond to the principal axes of the color space. The unique hue locations are the same as those in the CIELAB space under only the reference conditions. Example hue composition values are listed in table II in italics.

In some applications, such as the image color manipulation required for gamut mapping, it might be desirable to change colors along lines of

constant saturation rather than constant chroma. Wolski, Allebach, and Bouman²² have proposed such a technique. Saturation is defined as colorfulness relative to brightness, chroma is defined as colorfulness relative to the brightness of a white, and lightness is defined as brightness relative to the brightness of a white. Therefore saturation can be defined as chroma relative to lightness. Chroma, C^R , and lightness, L^R , are already defined in RLAB, thus saturation, s^R , is defined as shown in Eq. 16.

$$s^R = C^R / L^R \quad (16)$$

The inversion of the revised RLAB equations is illustrated in Appendix A.

Step-By-Step Calculation Procedure

The computation of RLAB values is accomplished using the above equations according to the following steps:

Step 1. Obtain the colorimetric data for the test and adapting stimuli and the absolute luminance of the adapting stimulus. Decide on the discounting-the-illuminant factor and the exponent (based on surround relative luminance).

Step 2. Calculate the chromatic adaptation matrix, A , using Eqs. 5-8.

Step 3. Calculate the reference tristimulus values using Eq. 9 and the A matrix derived in step 2.

Step 4. Calculate the RLAB parameters, L^R , a^R , and b^R using Eqs. 11-13.

Step 5. Use a^R and b^R to calculate C^R and h^R using Eqs. 14 and 15.

Step 6. Use h^R and Table II to determine H^R .

Step 7. Calculate s^R using C^R and L^R and Eq. 16.

Example input data and calculated values are given in Table III for 3 different cases of the RLAB equations. The 3 cases include 3 different levels of discounting-the-illuminant and 3 different surround conditions (i.e. exponents).

COLOR-DIFFERENCE SPECIFICATION

Since the RLAB color space is based on CIELAB and is essentially identical to CIELAB for the reference viewing conditions, it provides a convenient and familiar space for color-difference measurement. The normal E^* equations can be used to provide values similar to CIELAB E^*_{ab} . More complex color difference equations such as CMC or CIE94 can also be used with quite predictable results. In addition, since RLAB provides a more accurate transformation across viewing conditions it might be substantially more useful for comparing color-differences across viewing conditions than CIELAB. This could be applied to problems such as color rendering of light sources or calculating indices of metamerism.

COMPARISON OF NEW AND OLD RLAB EQUATIONS

To compare the new and old RLAB equations (only the steps after the adaptation transform), a sample of 125 colors was generated (5 levels each of X, Y, and Z uniformly spaced from 0 to 100). The RLAB coordinates of each of

these colors were calculated with both the old and new equations and then the RLAB (*i.e.* CIELAB) color differences between the old and new predictions were calculated. For an average surround the mean color difference was 6.2 units with a maximum of 12.2. For dim and dark surrounds the mean color differences were 5.5 and 4.9 with maximums of 11.4 and 10.6 respectively. While these changes might seem large, they are not significant when compared to the inter-observer variability in color-appearance judgements which can often exceed 20 CIELAB units¹⁷ and the differences between similarly-performing color-appearance models which are even larger. It should also be noted that the gamut of the 5X5X5 XYZ sampling (a simulation) far exceeds the gamut of physically realizable colors, thus producing a more rigorous comparison of the equations. Lastly, when using the new equations for reproduction (*i.e.* XYZ to RLAB for original and RLAB to XYZ for reproduction), they are essentially identical to the old equations for changes in surround.

A quantitative comparison of the performance of the new and old RLAB equations has been completed as part of the activity of CIE TC1-34, *Testing Colour-Appearance Models*, using an extensive data set collected by the Color Science Association of Japan (CSAJ).²³ Table IV contains the RMS color differences (E^*_{ab}) between the predicted and visually determined corresponding colors for three of the CSAJ experiments. The performance of the refined RLAB equations is unchanged for the chromatic-adaptation experiment, worse for the Hunt-effect experiment due to the removal of the C

matrix, and better for the Stevens-effect experiment, also due to the removal of the **C** matrix. While the lack of ability to predict the Hunt effect is a theoretical limitation of the new RLAB equations, it is not a practical limitation, since gamut-mapping constraints in color reproduction eliminate the possibility of reproducing images according to Hunt-effect predictions. Table IV also shows that the performance of the RLAB model is comparable to that of the Hunt model⁹ for the CSAJ data.

CONCLUSION

The RLAB color-appearance space performs as well as, or better than, more complex appearance models in imaging applications. This is likely due to the complex nature of image-color appearance judgements in comparison with judgements of simple color patches. The added complexity in other appearance models might be useful for predicting subtle color-appearance effects. However, these effects are apparently masked in image judgements. The RLAB equations have been simplified while at the same time improving their performance for all types of applications.

The Hunt model performed very well in experiment 2 on simple patches. Thus it is surprising that it did not perform equally well in other situations. One reason for this is some ambiguity in deciding the values of the various parameters in the Hunt model for a particular application. Also, it is likely that appearance judgements for images are based not only on the accuracy of individual colors, but on the relationships between colors (e.g.

image contrast). In the experiments described in this article, the Hunt model was implemented exactly as published.⁹ However, it is clear that the Hunt model can perform as well as the RLAB model if its various parameters are optimized to the particular viewing conditions.¹⁷ An advantage of the RLAB model is that its simplicity leaves little room for ambiguity in its implementation.

ACKNOWLEDGEMENTS

This research was supported by the NSF-NYS/IUCRC and NYSSTF-CAT Center for Electronic Imaging Systems. The author thanks Karen Braun, Audrey Lester, Taek Kim, and Elizabeth Pirrotta for their efforts setting up and completing the various psychophysical experiments.

REFERENCES

1. M.D. Fairchild, Some Hidden Requirements for Device-Independent Color Imaging, *SID International Symposium*, 865-868(1994).
2. M. D. Fairchild, and R. S. Berns, Image Color-Appearance Specification through Extension of CIELAB, *Color Res. Appl.* **18**, 178-190(1993).
3. CIE, *Colorimetry*, CIE Publication 15.2, Vienna (1986).
4. M. D. Fairchild, Formulation and Testing of an Incomplete-Chromatic-Adaptation Model, *Color Res. Appl.* **16**, 243-250(1993).
5. M. D. Fairchild, Considering the Surround in Device-Independent Color Imaging, *Color Res. Appl.* **20**, in press(1995).

6. T.G. Kim, R. S. Berns, and M. D. Fairchild, Comparing Appearance Models using Pictorial Images, *IS&T/SID Color Imaging Conference*, 72-77 (1993).
7. M.D. Fairchild, E. Pirrotta, and T.G. Kim, Successive-Ganzfeld Haplosopic Viewing Technique for Color-Appearance Research, *Color Res. Appl.* **19**, 214-221(1994).
8. J. v. Kries, Chromatic adaptation, *Festschrift der Albrecht-Ludwig Universität, Fribourg, 1902* (Translation: D.L. MacAdam, *Sources of Color Science*, MIT Press, Cambridge, 1970.).
9. R.W.G. Hunt, An Improved Predictor of Colourfulness in a Model of Color Vision, *Color Res. Appl.* **19**, 23-26(1994).
10. Y. Nayatani, K. Takahama, H. Sobagaki, and K. Hashimoto, Color-Appearance Model and Chromatic Adaptation Transform, *Color Res. Appl.* **15**, 210-221(1990).
11. E. Pirrotta, Testing Chromatic Adaptation Models using Object Colors, M.S. Thesis, Rochester Institute of Technology, (1994).
12. M.D. Fairchild, Visual Evaluation and Evolution of the RLAB Color Space, *IS&T/SID 2nd Color Imaging Conference, Scottsdale*, 9-13(1994).
13. K. Braun and M.D. Fairchild, Viewing Environments for Cross-Media Image Comparisons, *IS&T's 47th Annual Conference/ICPS*, 391-396(1994).
14. K.M. Braun, M.D. Fairchild, and P.J. Alessi, Viewing Environments for Cross-Media Image Comparisons, *Color Res. Appl.* **20**, in press(1995).

15. M.D. Fairchild, R.S. Berns, A.A. Lester, and H.K. Shin, Accurate Color Reproduction of CRT-Displayed Images as Projected 35mm Slides, *IS&T/SID 2nd Color Imaging Conference, Scottsdale*, 69-73(1994).
16. R.W.G. Hunt, *The Reproduction of Colour in Photography, Printing, and Television*, 4th Ed., Fountain Press, England, 254(1987).
17. R.W.G. Hunt and M.R. Luo, Evaluation of a Model of Color Vision by Magnitude Scalings: Discussion of Collected Results, *Color Res. Appl.* **19**, 27-33(1994).
18. N. Katoh, Practical Method for Appearance Match between Soft Copy and Hard Copy, in *Device-Independent Color Imaging*, SPIE Vol. 2170, 170-181(1994).
19. M.D. Fairchild, Chromatic Adaptation and Color Constancy, in *Advances in Color Vision Technical Digest*, Vol. 4 of the OSA Technical Digest Series (Optical Society of America, Washington, D.C.), 112-114(1992).
20. A. Hard and L. Sivik, NCS-Natural Color System: A Swedish Standard for Color Notation, *Color Res. Appl.* **6**, 129-138(1981).
21. P. Steen, Experiments with Estimation of Perceptive Qualitative Color Attributes, *AIC Color 69*, Stockholm, 369-376(1969).
22. M. Wolski, J.P. Allebach, and C.A. Bouman, Gamut Mapping: Squeezing the Most out of Your Color System, *IS&T/SID 2nd Color Imaging Conference, Scottsdale*, 89-92(1994).

23. L. Mori, H. Sobagaki, H. Komatsubara and K. Ikeda, Field trials on CIE chromatic adaptation formula, *Proceedings of the CIE 22nd Session*, 55-58 (1991).

APPENDIX A: INVERSE RLAB EQUATIONS

In typical color reproduction applications it is not enough to know the appearance of image elements; it is necessary to reproduce those appearances in a second set of viewing conditions. To accomplish this, one must be able to calculate CIE tristimulus values, XYZ, from the appearance parameters, $L^R a^R b^R$, and the definition of the new viewing conditions. These tristimulus values are then used, along with the imaging-device characterization, to determine device color signals such as RGB or CMYK. The following equations outline how to calculate CIE tristimulus values from RLAB $L^R a^R b^R$. If starting with $L^R C^R h^R$, one must first transform back to $L^R a^R b^R$ using the usual transformation from cylindrical to rectangular coordinates.

The reference tristimulus values are calculated from the RLAB parameters using Eqs. A1-A3 with an exponent, n , appropriate for the second viewing condition.

$$Y_{\text{ref}} = \frac{L^R}{100}^{1/n} \quad (\text{A1})$$

$$X_{\text{ref}} = \frac{a^R}{430} - (Y_{\text{ref}})^{1/n} \quad (\text{A2})$$

$$Z_{\text{ref}} = (Y_{\text{ref}})^{1/n} - \frac{b^R}{170} \quad (\text{A3})$$

The reference tristimulus values are then transformed to tristimulus values for the second viewing condition using Eq. A4 with an **A** matrix calculated for the second viewing conditions.

$$\begin{bmatrix} X \\ Y \\ Z \end{bmatrix} = (\mathbf{RAM})^{-1} \begin{bmatrix} X_{\text{ref}} \\ Y_{\text{ref}} \\ Z_{\text{ref}} \end{bmatrix} \quad (\text{A4})$$

LIST OF TABLES (HEADINGS)

Table I. Rank order of model performance in each of the 4 visual experiments.

Table II. Data for conversion from hue angle to hue composition.

Table III. Example input data and calculated results.

Table IV. RMS E^*_{ab} between predicted and experimental corresponding colors for three CSAJ experiments.

Table I. Rank order of model performance in each of the 4 visual experiments.

Model	Exp.1	Exp.2	Exp.3	Exp.4
RLAB ²	1	5	1	1
CIELAB ³	1	2	2	2
von Kries ⁸	1	2	3	2
Hunt ⁹	1	1	4	4
Nayatani ¹⁰	5	2	5	(5)

Table II. Data for conversion from hue angle to hue composition.

h^R	R	B	G	Y	H^R
24	100	0	0	0	R
90	0	0	0	100	Y
162	0	0	100	0	G
180	0	21.4	78.6	0	<i>B79G</i>
246	0	100	0	0	B
270	17.4	82.6	0	0	<i>R83B</i>
0	82.6	17.4	0	0	<i>R17B</i>
24	100	0	0	0	R

Table III. Example input data and calculated results.

	Case 1	Case 2	Case 3
X	66.76	66.76	66.76
Y	45.02	45.02	45.02
Z	2.07	2.07	2.07
X _n	109.85	109.85	109.85
Y _n	100.00	100.00	100.00
Z _n	35.58	35.58	35.58
Y _n (Abs.)	150 cd/m ²	150 cd/m ²	150 cd/m ²
Discounting	No	Partial	Yes
D	0.0	0.5	1.0
Surround	Dark	Dim	Average
	1/3.5	1/2.9	1/2.3
L ^R	80.79	76.48	70.32
a ^R	28.40	29.86	31.37
b ^R	66.89	68.69	70.20
C ^R	72.67	74.90	76.89
s ^R	0.900	0.979	1.093
h ^R	67.0°	66.5°	65.9°
H ^R	Y35R	Y36R	Y37R

Table IV. RMS E^*_{ab} between predicted and experimental corresponding colors for three CSAJ experiments.

Experiment	Old RLAB	New RLAB	Hunt
Chromatic Adaptation	7.2	7.2	7.3
Hunt Effect	9.5	13.3	8.5
Stevens Effect	8.8	5.9	4.8

LIST OF FIGURES (CAPTIONS)

Figure 1. Lightness, L^R , deviations between new and old RLAB compression functions for dark, dim, and average surrounds.

Figure 2. The relationship between perceptual unique hues (based on NCS) and the RLAB a^R and b^R dimensions.

Figure 1.

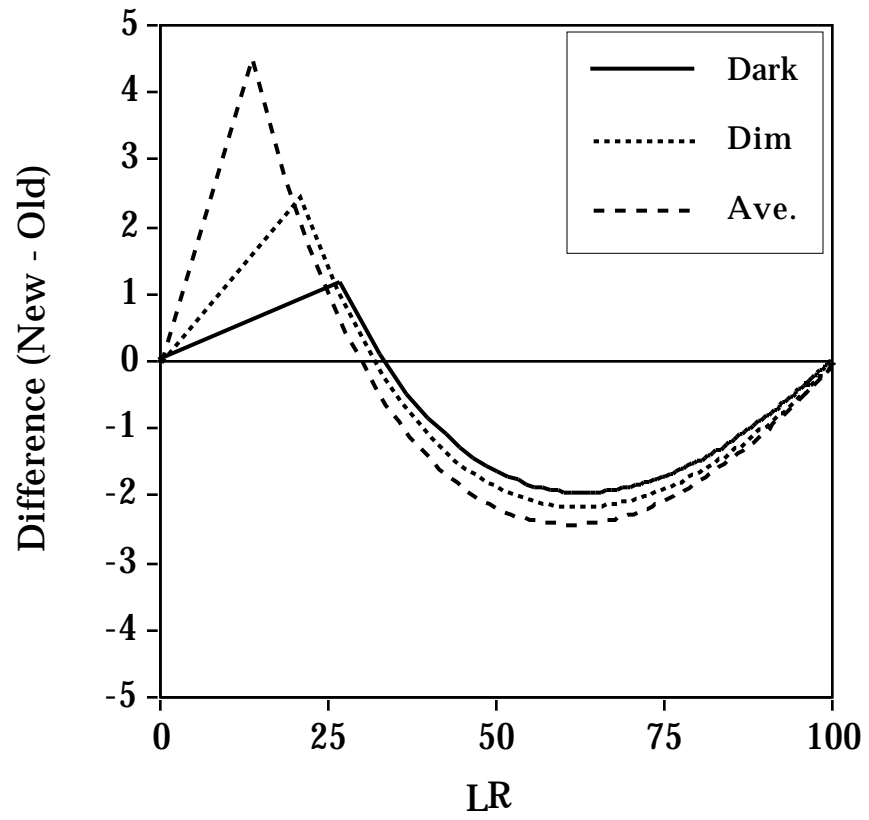


Figure 2.

